BIOCHEMISTRY
including biophysical chemistry & molecular biology

Article

pubs.acs.org/biochemistry

Metal Binding at the *Deinococcus radiodurans* Dps-1 N-Terminal Metal Site Controls Dodecameric Assembly and DNA Binding

Khoa Huynh Nguyen and Anne Grove*

Department of Biological Sciences, Louisiana State University, Baton Rouge, Louisiana 70803, United States

ABSTRACT: The prokaryotic DNA protection during starvation (Dps) proteins typically protect macromolecules against damaging agents via physical association with DNA and by oxidizing and sequestering iron. However, *Deinococcus radiodurans* Dps-1, which binds DNA with high affinity, fails to protect DNA against hydroxyl radicals due to iron leakage from the core, raising the question of how $^{\bullet}$OH-mediated damage to Dps-1-bound DNA is avoided. As shown here, Mn(II) inhibits ferroxidase activity, suggesting that ferroxidation may be prevented *in vivo* as *D. radiodurans* accumulates a high ratio of Mn:Fe. Dps-1 has an N-terminal extension with a unique metal-binding site, an extension that has been proposed to be important for DNA binding and dodecameric assembly. Electrophoretic mobility shift assays show that Mn(II) restores DNA binding to bipyridyl-treated Dps-1, whereas Fe(II) fails to do so in the presence of H_2O_2, thus preventing DNA binding under conditions of ongoing ferroxidase activity. We also show that disruption of the N-terminal metal site leads to a significant reduction in DNA binding and to compromised oligomeric assembly, with the mutant protein assembling into a hexamer in the presence of divalent metal. We propose that securing the N-terminal loop by metal binding is required to initiate dodecameric assembly by contacting the neighboring dimer and that the absence of such optimal contacts results in formation of a hexameric assembly intermediate in which three dimers associate about one of the 3-fold axes. Once dodecameric Dps-1 is assembled, metal binding no longer affects oligomeric state; instead, differential metal binding controls DNA interaction under conditions of oxidative stress.

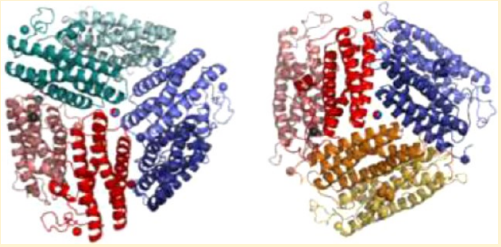

Oxidative stress is a condition that is generated by various environmental hazards such as radiation and desiccation as well as by endogenous conditions, including nutritional stress and starvation. Under these circumstances, large amounts of reactive oxygen species (ROS) such as H_2O_2, $^{\bullet}$OH, and $^{\bullet}O_2^-$ are produced that can damage cellular components. Furthermore, these partially reduced oxygen species can be transformed into a more toxic form; for example, H_2O_2 can react with the transition metal Fe(II) to produce the highly toxic $^{\bullet}$OH. In bacteria, there are many different proteins that can protect against ROS. Some proteins, such as catalases and superoxide dismutases, can provide protection by detoxifying these species and other proteins also provide physical protection.[1−3] One prominent example of the latter is the Dps (DNA protection during starvation) protein.

Most Dps-family proteins protect the cells through two mechanisms: by physically binding and shielding the DNA against damaging agents and by sequestering and oxidizing Fe(II) to block the formation of $^{\bullet}$OH.[4−7] Dps proteins possess a structure that is similar to that of the iron storage protein ferritin. However, Dps is smaller than ferritin in that it has only 12 subunits and assembles with 23 tetrahedral symmetry, compared to the 24 subunits of ferritin, which assemble with 432 octahedral symmetry. Furthermore, each ferritin subunit has its own ferroxidase center while in most Dps homologues, an active ferroxidase center is localized between two subunits.[8,9] These ferroxidase sites catalyze the conversion of ferrous iron to Fe^{3+}, but unlike ferritin, Dps-family proteins generally prefer H_2O_2 over molecular oxygen as the oxidant; this distinction is important as it allows Dps to inactivate Fe^{2+} and H_2O_2 simultaneously. The implication is also that the primary function of Dps proteins is to prevent the hydroxyl radical production that would occur by environmental oxidation of Fe^{2+}. Like ferritin, Dps ultimately accumulates iron in its central cavity to generate a hydrous ferric oxide mineral core; the smaller size of its internal cavity results in accumulation of ∼500 Fe compared to the ∼4500 Fe per ferritin shell. Several residues are conserved among Dps proteins including the ones that are involved in coordinating the iron at the ferroxidase center; however, N- and C-terminal extensions beyond the four-helix bundle subunit have variable length. These extensions have been shown to contribute greatly to DNA binding and oligomerization of some Dps homologues.[10−12]

The Gram-positive bacterium *Deinococcus radiodurans* is known for its extreme resistance to various stress conditions including UV and ionizing radiation, a resistance thought to correlate with its resistance to desiccation.[13] It can survive up to thousand grays of radiation without losing viability. In other bacteria such as *E. coli*, such exposure would be lethal due to the massive damage to macromolecules.[14,15] One potential contributor to the extreme resistance characteristic of *D. radiodurans* is its relatively high Mn/Fe ratio;[16] while Fe(II) can enhance the toxicity of ROS, Mn(II) has been proposed to provide protection by blocking the ROS-mediated oxidation of

Received: May 29, 2012
Revised: July 27, 2012
Published: July 31, 2012

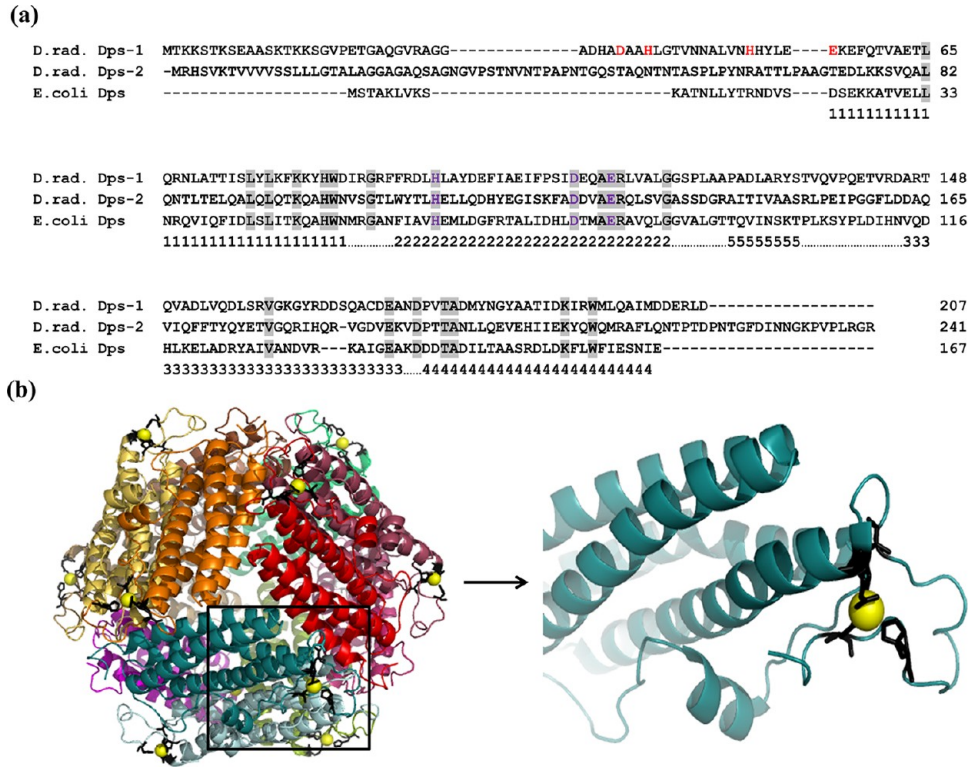

Figure 1. Sequence alignment. (a) Alignment of *D. radiodurans* (*D. rad.*) Dps-1 and Dps-2 and *E. coli* Dps. Gray shading identifies conserved amino acids. The numbers 1−5 below the alignment represent the helical segments in each subunit. Residues involved in coordinating the metal at the ferroxidase center are highlighted in purple. Residues involved in coordinating the N-terminal metal in Dps-1 are highlighted in red. (b) Left panel shows the quaternary structure of Dps-1. Each monomer is represented by a different color. The right panel is an enlarged view of the N-terminal metal binding site with the residues coordinating the metal highlighted in black (Asp36, His39, His50, and Glu55). The metals at the N-terminus are represented by yellow spheres.

proteins. In *D. radiodurans*, Mn(II) is found throughout the cells but Fe(II) is concentrated near the area between dividing cells.[17]

D. radiodurans encodes two Dps proteins, Dps-1 and Dps-2.[18] Both Dps-1 and Dps-2 have an N-terminal extension that is much longer than that of other Dps homologues; however, part of the N-terminal extension of Dps-2 is a predicted signal peptide. One of the unique features of Dps-1 is that it fails to protect against ROS despite being able to bind DNA with high affinity, a property inferred to derive from iron leaking from its mineral core.[19,20] Such iron leakage would be expected to result in DNA damage were it to occur while Dps-1 is bound to DNA. Experiments reported below provide a possible mechanism by which the two functions of Dps-1 may be separated to prevent $^{\bullet}$OH-mediated damage to Dps-1-bound DNA. The crystal structure of Dps-1 (Figure 1) reveals not only the expected four-helix bundle subunit but also four metal-binding sites (Table 1). For two of the metal-binding sites, the iron entry channel and the iron exit channel, divalent metals are coordinated mainly by negatively charged residues from three adjoining subunits. The 23 symmetry of Dps-1 leads to two nonequivalent 3-fold interfaces. One such interface is the N-terminal ferritin-like channel that shares similar packing with ferritin and is lined with negatively charged residues; this interface corresponds to the iron entry channel. The other is the C-terminal pore that is unique to Dps proteins and is inferred to function as the iron exit channel in Dps-1. Another metal site is at the ferroxidase center with ligands from two subunits, created by 2-fold rotational symmetry. Finally, Dps-1 contains a unique metal binding site at the base of the N-terminal extension.[20,21] Here we show that this metal site is required to initiate dodecameric assembly and that it also contributes greatly to DNA binding. Our data suggest that disruption of the N-terminal metal site results in suboptimal assembly of Dps-1 in which the protein forms a hemispherical hexamer and that occupancy of the N-terminal metal site is required for DNA binding.

Table 1. Four Metal Sites in Dps-1[a]

	Location	Symmetry axis	Coordinating residues
1	N-terminus	N/A	D36, H39, H50, E55
2	Ferroxidase center	2-fold	H83, D110, E114
3	Iron entry	3-fold	D181
4	Iron exit	3-fold	E100

[a]Numbering of metal sites corresponds to their identification in the Dps-1 structure (PDB 2F7N). The symmetry leads to two types of nonequivalent 3-fold interfaces, corresponding to the iron entry and exit channels. Dps-1 subunits are represented by rectangles and filled circles represent metal sites.

MATERIALS AND METHODS

Cloning, Overexpression, and Purification of Dps-1, Dps-dn, and Dps-HE. Wild-type Dps-1 and Dps-dn lacking

dx.doi.org/10.1021/bi300703x | *Biochemistry* 2012, 51, 6679−6689

the N-terminal extension were purified and characterized as previously described.[11,19] For the Dps-HE mutant, the following primers were used to introduce the mutations (CAC to AGC and GAA to CAA; mutagenic codons underlined) by whole plasmid amplification of plasmid harboring the Dps-1 gene: 5′-CACCAGCCACTACCTGGAACAAAAAG-3′ and 5′-ACGAGCGCGTTGTTCACG-3′. The PCR product was transformed into *E. coli* TOP10 cells, and the resulting plasmid confirmed by sequencing. The mutant Dps-1 (Dps-HE) was overexpressed in *E. coli* BL21(DE3)pLysS grown in LB at 37 °C with 1.0 mM isopropyl-β-D-thiogalactopyranoside for 2 h. Cells were lysed in lysis buffer [50 mM Tris, 0.25 M NaCl, 5 mM EDTA, 5% glycerol, 5 mM β-mercaptoethanol, 0.1 mM phenylmethylsulfonyl fluoride (PMSF), and 0.5 mg/mL lysozyme], followed by dialysis against buffer A [20 mM Tris-HCl (pH 7.5), 50 mM KCl, 5% glycerol, 1 mM EDTA, 5 mM β-mercaptoethanol, 0.2 mM PMSF]. The dialysate was applied to a heparin−agarose column equilibrated in buffer A. The protein was eluted with a linear gradient from 50 mM to 1 M KCl in buffer A. The elutions from the heparin column that contain the mutant protein were collected and dialyzed against buffer A and applied to a diethylaminoethyl (DEAE)−Sepharose column equilibrated in buffer A and eluted with a linear gradient from 50 mM to1 M KCl in buffer A. The elutions from the DEAE−Sepharose column that contain the mutant protein were collected and dialyzed against buffer A and applied to a carboxylmethyl (CM)−cellulose column equilibrated in buffer A and eluted with a linear gradient from 50 mM to 1 M KCl in buffer A. Protein concentration was determined by staining of SDS polyacrylamide gels with Coomassie brilliant blue using bovine serum albumin (BSA) as a standard and by using the Micro BCA Protein Assay Kit (Pierce). Purified proteins were judged to be >95% pure based on Coomassie-stained SDS-PAGE gels.

Native Polyacrylamide Gel Electrophoresis. The oligomeric state of the mutant Dps-HE was visualized on a 5% nondenaturing acrylamide gels. The gel components were the same as the running gel of SDS-PAGE according to the method of Laemmli, except SDS was not included. The gel was run in a buffer composed of 375 mM Tris-HCl, pH 8.7. At least three independent experiments were performed to confirm migration.

Gel Filtration. The entire gel filtration experiment was done at 4 °C. HiLoad 16/60 Superdex 30 prep grade column (bed length 60 cm, inner diameter 16 mm; GE Healthcare) was first washed with 1 column volume of buffer AP, pH 8.0 (50 mM $Na_xH_yPO_4$, 10 mM imidazole, 10% glycerol), and then with 2 column volumes of buffer BP, pH 8.0 (50 mM $Na_xH_yPO_4$, 300 mM NaCl, 10 mM imidazole, 10% glycerol). The gel filtration standard (Bio-Rad), which is a mixture of bovine thyroglobulin (670 kDa), bovine γ-globulin (158 kDa), chicken ovalbumin (44 kDa), horse myoglobin (17 kDa), and vitamin B-12 (1.35 kDa), was run to calibrate the column. 3 mg/mL Dps-HE was applied to the gel filtration column, and the protein was eluted with a flow rate of 0.5 mL/min.

Thermal Stability. Dps-1 or bipyridyl-treated Dps-1 (Dps-1 incubated with 50 mM bipyridyl for 20 min at 4 °C, followed by dialysis) was diluted to 10 μM in a buffer containing 50 mM Tris pH 8.0, 100 mM NaCl, and 5X SYPRO Orange (Invitrogen). Fluorescence emission resulting from dye binding to unfolded protein was measured over a temperature range of 1−90 °C in 1 deg increments for 45 s using an Applied Biosystems 7500 Real-Time PCR System using the SYBR green filter. The correction for the total fluorescence yield was made using reactions without protein. The resulting data were exported to Sigma Plot 9, and the sigmoidal part of the curve was fit to a four-parameter sigmoidal equation. Errors on the calculated T_m reflect standard deviation from two independent experiments.

Electrophoretic Mobility Shift Assays. Oligonucleotides used to generate duplex DNA were purchased and purified by denaturing polyacrylamide gel electrophoresis. One strand was ^{32}P-labeled at the 5′-end with T4 polynucleotide kinase. Equimolar amounts of complementary oligonucleotides were mixed, heated to 90 °C, and slowly cooled to 4 °C to form duplex DNA.

Electrophoretic mobility shift assays (EMSA) were performed using 10% polyacrylamide gels [39:1 (w/w) acrylamide:bis(acrylamide)] in 0.5X TBE (50 mM Tris borate, 1 mM EDTA). Gels were prerun for 30 min at 175 V at 23 °C before loading the samples with the power on. DNA and protein were incubated for 1 h at room temperature in binding buffer containing 20 mM Tris HCl (pH 8.0) and 500 mM NaCl. Each reaction contained 5 fmol of 26 bp DNA with increasing concentrations of Dps-1 or Dps-HE in a total reaction of 10 μL. The sequence of 26 bp DNA was 5′-CGTGACTACTATAAATAGATGATCCG-3′. After electrophoresis, gels were dried and protein−DNA complexes and free DNA were quantified by phosphorimaging using software supplied by the manufacturer (ImageQuant 1.1). For K_d determination, the percentage of complex formation was plotted against [Dps], and data were fit to the Hill equation, $f = f_{max}[Dps]^n/(K_d + [Dps]^n)$, where f is fractional saturation, [Dps] is the protein concentration, K_d reflects the apparent equilibrium dissociation constant, and n is the Hill coefficient. Error bars represent standard deviation from four replicates.

Effect of Divalent Metal Ions on DNA Binding. In order to obtain a metal-free Dps-1 and Dps-HE, the proteins were incubated with 50 mM bipyridyl for 20 min at 4 °C. The bipyridyl-treated protein was dialyzed against a high salt buffer (10 mM Tris-HCl, pH 8.0, 500 mM KCl, 5% (v/v) glycerol, 5 mM β-mercaptoethanol, and 0.2 mM PMSF) at 4 °C for 2 h to remove the bipyridyl. DNA (2.5 fmol) was then incubated with varying concentration of bipyridyl-treated Dps-1 with or without the addition of metals (80 nM $Fe(NH_4)_2(SO_4)_2$, $MnCl_2$, or $CoCl_2$). For Dps-HE, 1 μM of $MnCl_2$ was used. Where indicated, 1 mM H_2O_2 was added. The reactions were analyzed on a 10% polyacrylamide gel (39:1 (w/w) acrylamide:bis(acrylamide)) in 0.5X TBE. After electrophoresis, the gel was dried, and protein−DNA complexes and free DNA were visualized by phosphorimaging. Experiments were repeated at least three times.

Ferroxidation. The kinetics of iron oxidation by Dps-1 was measured at 310 nm using an Agilent 8453 spectrophotometer. Dps-1 was diluted to 0.2 mg/mL and dialyzed against the reaction buffer, 20 mM Mops, pH 7.0, 100 mM NaCl. Prior to each experiment, fresh solution of ferrous ammonium sulfate and manganese chloride were prepared. Reactions contained 50 μM ferrous iron and 10 μM $MnCl_2$. Experiments were repeated three times. The kinetic data were plotted using Prizm.

Metal Binding by Dps-1 and Dps-HE. Dps-1 and Dps-HE (50 μg/mL) previously treated with bipyridyl as described above was incubated with 1 μM $CoCl_2$ following which excess metal was removed by dialysis. To denature the proteins, SDS was added, followed by incubation at 90 °C for 10 min. Samples were mixed with 125 μM of 4-(2-pyridylazo) resorcinol (PAR) in buffer A (20 mM Tris-HCl (pH 7.5), 100 mM KCl, 5% glycerol), and the absorbance from 320 to 675 nm was recorded

dx.doi.org/10.1021/bi300703x | *Biochemistry* 2012, 51, 6679−6689

using an Agilent 8453 spectrophotometer. Experiments were performed twice.

RESULTS

The N-Terminal Metal-Binding Site Is Required for Dodecameric Assembly. Alignment of the amino acid sequence of Dps-1 with that of other Dps homologues reveals significant homology. For example, residues involved in assembling the ferroxidase center at the interface between two subunits are completely conserved (Figure 1a), and Dps-1 exhibits the associated ferroxidase activity.[19] The main difference is the N-terminus that extends from the four-helix bundle core. Dps-1 has a lengthy N-terminal extension that has been shown to play an important role in oligomeric assembly and DNA binding. A unique feature of this extension is a metal-binding site in which a divalent metal ion is coordinated by Asp36, His39, and His50 from the N-terminus and Glu55 from the α1 helix (Figure 1b). When the entire N-terminal extension including the metal-binding site is deleted, the protein exists exclusively as a dimer (this mutant was named Dps-dn). In contrast, when the first 33 amino acids of the extension are deleted with the metal-binding site remaining intact, dodecameric assembly is unaffected. Based on this observation, occupancy of the metal-binding site was inferred to stabilize the resulting loop that contacts the neighboring dimer, contacts that must be required for oligomeric assembly.[11]

The Dps-1 interfaces were also analyzed using the Protein Interfaces, Surfaces, and Assemblies (PISA) server.[22] The PISA server uses parameters such as hydrogen-bonding, interface area, and solvation energy gain to analyze a given structure and predict the most thermodynamically stable assemblies. The PISA algorithm predicts several interfaces that contribute significantly to assembly, with the most significant contributions deriving from metal-coordination at the N-terminal metal site, followed by interactions of the resulting loop with an adjacent subunit and protein−protein contacts at the dimer interface (Table 2). Additional contributions derive from protein−protein interactions between subunits at the 3-fold axis that passes through the iron exit channels, from coordination of metals at the ferroxidase center and the iron entry channels, and from coordination of a sulfate molecule adjacent to the metal at the iron exit channels. Based on these predictions, disruption of the N-terminal metal site should severely compromise oligomerization of Dps-1 and/or stability of the dodecameric assembly.

Table 2. PISA Analysis Predicts Several Interfaces That Contribute to Assembly of Dps-1[a]

type of interaction	HB + SB	CSS
N-terminal Co^{2+} and protein subunit	0	0.415
N-terminal loop and adjacent subunit	18	0.385
dimer interface	26	0.326
adjacent subunits at 3-fold exit channel	16	0.101
Co^{2+} at iron entry channel	0	0.129
Co^{2+} at iron exit channel	0	0.094[b]
Co^{2+} at ferroxidase center/subunit 1	0	0.201
Co^{2+} at ferroxidase center/subunit 2	0	0.148

[a]aHB + SB, number of hydrogen bonds and salt bridges. CSS; complex formation significance score, an indicator of interface relevance to complex formation.[22] In addition to the listed interfaces, contacts to a sulfate molecule near the metal at the iron exit channel is also predicted to contribute to complex stability. [b]Not a significant contribution. Calculations done using the PISA server at www.ebi.ac.uk/msd-srv/prot_int/pistart.html in autoprocessing mode with PDB 2F7N.[20] Metal at the ferroxidase center is coordinated by two subunits, generating two distinct interfaces.

Removal of metals from dodecameric Dps-1 by bipyridyl does not alter the oligomeric state.[11] To assess the prediction from the PISA analysis that it would destabilize the assembly, we compared thermal stability of Dps-1 and bipyridyl-treated protein using SYPRO Orange as a fluorescent reporter of protein unfolding (Figure 2). Consistent with predictions, the melting temperature of Dps-1 of 65.0 ± 0.0 °C is reduced to 52.2 ± 0.1 °C on removal of metals.

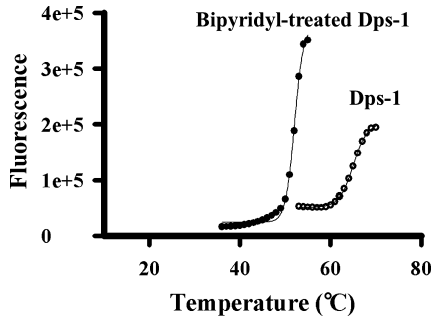

Figure 2. Thermal stability of Dps-1. Fluorescence emitted from SYPRO Orange upon binding to denatured protein measured as a function of temperature. Untreated Dps-1 (open symbol) and Dps-1 treated with bipyridyl (closed symbol).

Structuring of the metal-bound loop may also be required for DNA binding as evidenced by the failure of dodecameric Dps-1 to bind DNA when metals have been removed by bipyridyl treatment.[11] To address the function of the N-terminal metal-binding site directly, a mutant was created in which two of the four residues that coordinate the metal were mutated (His50 to Ser and Glu55 to Gln). The mutant protein named Dps-HE was successfully purified (Figure 3b, inset).

To define the role of the N-terminal metal site in dodecameric assembly, gel filtration was performed. These experiments reveal that Dps-HE (M_w ~ 23 kDa) elutes as an oligomer with a molecular weight of ~150 kDa, suggesting that it exists as a hexamer (Figure 3b,c). This is unusual because Dps homologues generally exist as a dimer, trimer, or dodecamer.[11,19,23] The incomplete oligomeric assembly of Dps-HE was confirmed by native gel electrophoresis. Full-length Dps-1 and Dps-dn (the mutant Dps-1 that lacks the first 55 amino acids, including the metal-binding site) were used as controls because both proteins were previously shown by gel filtration to exist exclusively as a dodecamer and a dimer, respectively.[11] As seen in Figure 3d, dodecameric Dps-1 fails to migrate from the well (lane 1) while dimeric Dps-dn migrates a significant distance (lane 6). Dps-HE migrates in between Dps-1 and Dps-dn, which is consistent with a hexameric assembly (lanes 2 and 8).

An excess of Mn(II) was added to Dps-HE to see if it can restore dodecamer assembly. Mn(II) was chosen because *D. radiodurans* has an unusually high ratio of manganese to iron, a feature proposed to contribute to its radiation resistance. However, addition of Mn(II) did not cause Dps-HE to oligomerize to a dodecamer (lanes 3−4). Instead, removal of metals by chelation with bipyridyl causes significant disassembly into dimers (lanes 5 and 7); longer incubation of Dps-HE with bipyridyl increases the fraction of protein that exists as a dimer (data not shown), suggesting slow disassembly on removal of metals. Notably, when metals were added to the bipyridyl-treated

dx.doi.org/10.1021/bi300703x | *Biochemistry* 2012, 51, 6679−6689

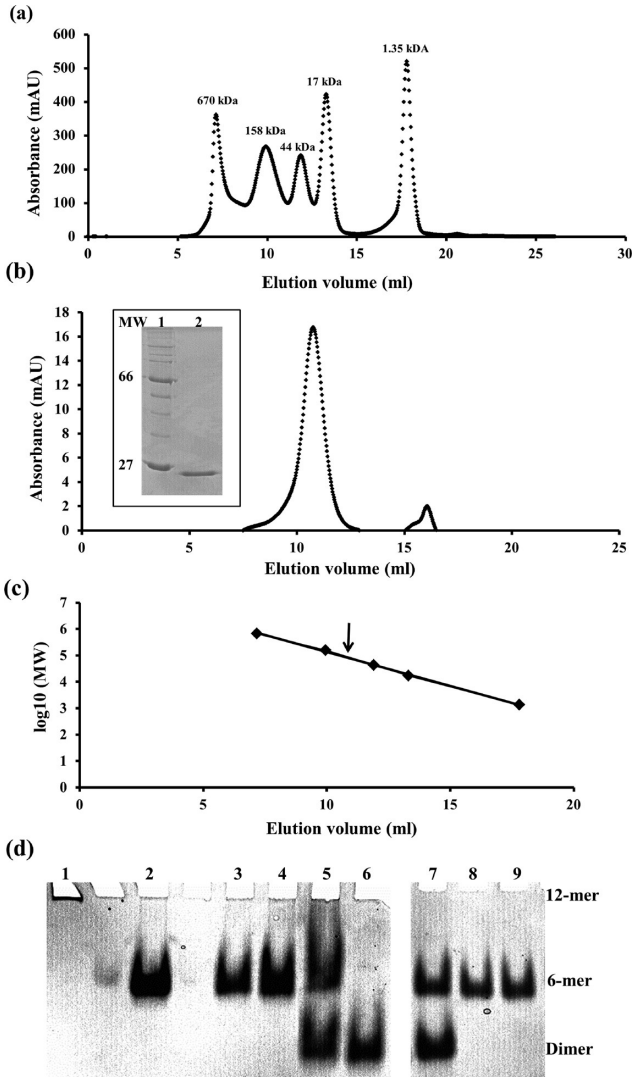

Figure 3. Oligomeric state of Dps-HE. (a) The molecular mass standards used to standardize the FPLC column. (b) The elution pattern of Dps-HE. Inset shows SDS PAGE of purified Dps-HE (lane 2). (c) The logarithm of molecular mass as a function of elution volume. The arrow represents the elution volume of Dps-HE. (d) Native gel showing the oligomeric state of Dps-1, Dps-HE, and Dps-dn. Lane 1 contains Dps-1, lanes 2 and 8 contain Dps-HE, lanes 3 and 4 contain Dps-HE with 800 and 400 nM Mn, respectively, lanes 5 and 7 contain bipyridyl-treated Dps-HE, lane 6 contains Dps-dn, and lane 9 contains bipyridyl-treated Dps-HE followed by addition of 800 nM Mn.

Dps-HE, the dimers reoligomerize to a hexamer (lane 9), indicating that hexameric assembly of Dps-HE is metal-dependent. Furthermore, glutaraldehyde-mediated cross-linking of Dps-HE and Dps-dn in the presence of excess metals also did not result in higher oligomeric states than a hexamer for Dps-HE and a dimer for Dps-dn (data not shown), suggesting that the failure to observe such higher oligomeric assemblies is not due to their instability during electrophoresis. While we cannot rule out the existence of oligomeric assemblies in solution that cannot be cross-linked, we consider this possibility unlikely since cross-linking of full-length Dps-1 reveals the expected dodecamer.[19] Collectively, these experiments point to a requirement for metal binding at the N-terminal metal site for complete oligomeric assembly. That neither Dps-HE nor Dps-dn assembles into higher-order oligomers in presence of Mn(II) also suggests that subunit coordination around a metal site at the 3-fold axes, whether at the iron entry or exit sites (Table 1), is insufficient to drive assembly in absence of other stabilizing interactions.

Dps-HE Binds Metals. Substitution of residues that coordinate metal at the N-terminal metal site results in incomplete oligomeric assembly, attesting to the involvement of this site in dodecamer formation. Yet the presence of divalent metal is still required for dimeric Dps-HE to form the larger oligomeric species seen in both gel filtration and native gels. To confirm that added metal indeed binds to the proteins, we used 4-(2-pyridylazo)resorcinol (PAR), which binds various divalent metals resulting in a diagnostic absorbance of the metal−PAR complex[24] to evaluate metal binding by Dps-1 and Dps-HE.

As shown in Figure 4a,b, uncomplexed PAR has an absorbance maximum at 416 nm (gray line), and addition of bipyridyl-treated native or denatured Dps-1 (Figure 4a) or Dps-HE (Figure 4b) (continuous and broken cyan lines, respectively) has no effect on the wavelength of maximal absorbance, indicating the absence of divalent metals from bipyridyl-treated proteins that can form a detectable complex with PAR. After incubation of bipyridyl-treated proteins with Co^{2+}, a shift in the peak absorbance to 508 nm is seen on incubation of PAR with denatured proteins (red broken line) while no absorbance peak at 508 nm is seen on incubation of PAR with native protein (red continuous line). This absorbance maximum is diagnostic of the Co(II)−PAR complex and shows that both proteins bind the divalent metal. We attempted to assess metal binding specifically to the N-terminal metal site; as this would require monomeric Dps-1, we conducted an experiment in which Dps-1 and Dps-HE were run on an SDS-PAGE gel followed by staining in a buffer containing PAR (addition of guanidine failed to disassemble the very stable Dps-1). This attempt was unsuccessful because the metals were no longer associated with the monomeric proteins, indicating that the N-terminal metal site was unfolded by exposure to SDS (data not shown). Significantly, the evidence for metal binding by both bipyridyl-treated Dps-1 and Dps-HE supports the observed metal-dependent assembly of Dps-HE hexamers and the metal-dependent DNA binding discussed below.

The N-Terminal Metal-Binding Site Affects DNA Binding. Both dimeric and dodecameric forms of Dps-1 bind DNA, but dimeric Dps-1 has very low affinity.[19] Deletion of the N-terminal extension obliterates the ability of Dps-1 to bind DNA whether or not the N-terminal metal site is retained, indicating that sequence preceding the metal site is required for DNA binding.[11] If occupancy of the N-terminal metal site contributes to structuring the N-terminal extension for optimal DNA binding, then DNA binding by Dps-HE should be compromised. Electrophoretic mobility shift assays (EMSA) show that Dps-HE indeed binds DNA with a much lower affinity compared to full length Dps-1. There is no clear complex formation unless DNA is incubated with 50 nM of Dps-HE (Figure 5b). Furthermore, the complexes appear to be unstable and dissociate during electrophoresis as evidenced by the smeared appearance of protein-bound DNA. In contrast, Dps-1 forms complexes with DNA at ~0.5 nM dodecameric protein (Figure 5a). Quantitation of binding isotherms show that Dps-HE binds DNA with a K_d of 120 ± 8 nM, which is more than 100-fold higher compared to wild-type Dps-1 (K_d = 0.5 ± 0.1 nM) (Figure 5c,d). The Hill coefficient for hexameric Dps-HE is <1, suggesting that there is no positive cooperativity as opposed to wild-type Dps-1, which binds DNA cooperatively. These data are consistent with the hypothesis that occupancy of

dx.doi.org/10.1021/bi300703x | Biochemistry 2012, 51, 6679−6689

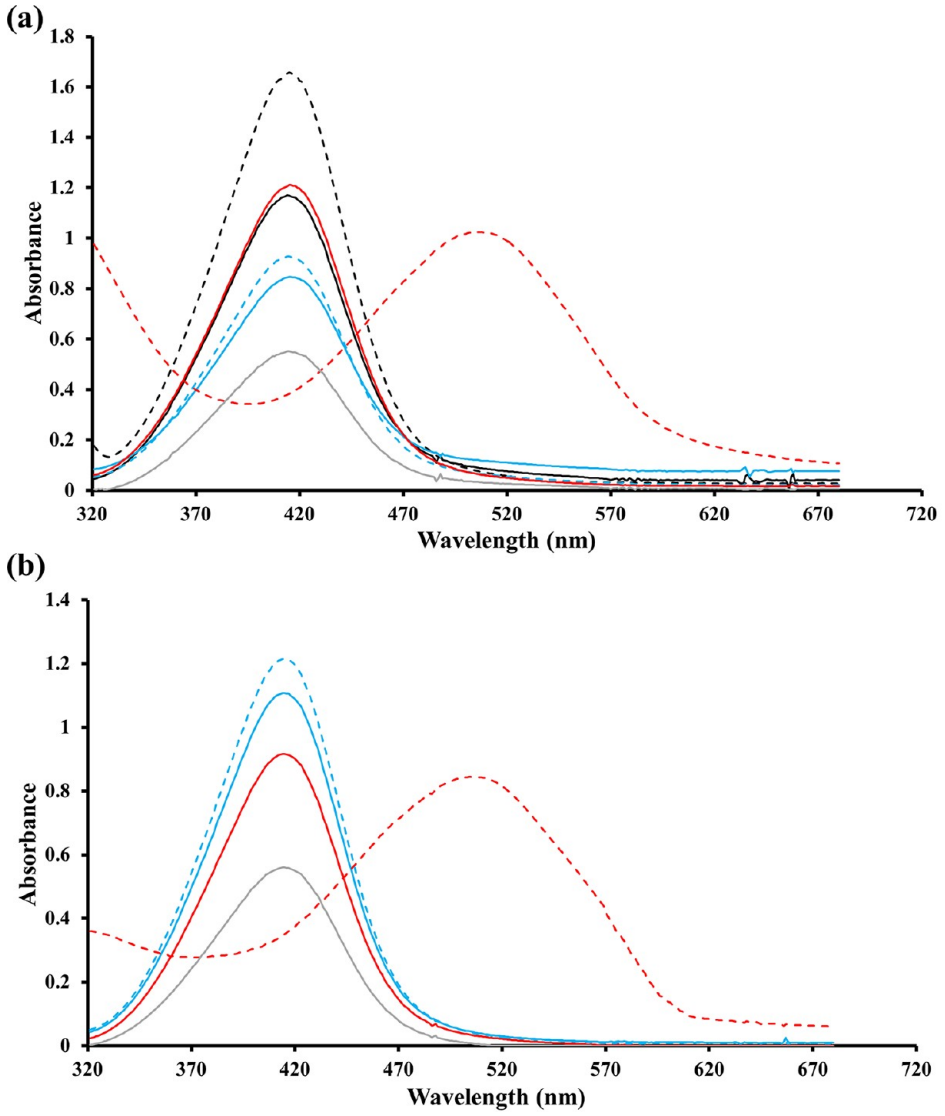

Figure 4. Metal binding by Dps-1 and Dps-HE. (a) Absorption spectrum of native, untreated Dps-1 (black continuous line), denatured, untreated Dps-1 (black broken line), bipyridyl-treated native Dps-1 (cyan line), bipyridyl-treated denatured Dps-1 (cyan broken line), metal-containing native Dps-1 (red line), metal-containing denatured Dps-1 (red broken line), and buffer with PAR (gray line). (b) Absorption spectrum of bipyridyl-treated native Dps-HE (cyan line), bipyridyl-treated denatured Dps-HE (cyan broken line), metal-containing native Dps-HE (red line), metal-containing denatured Dps-HE (red broken line), and buffer with PAR and SDS (gray line).

the metal sites is required to orient the N-terminal extensions for optimal DNA binding.

Effect of Metals on DNA Binding by Dps-1 and Dps-HE. Removal of metals from dodecameric Dps-1 destroys DNA binding (inferred to be due to removal of metal from the N-terminal site) but it does not disrupt oligomeric assembly, and subsequent addition of metal (Co(II)) restores DNA binding.[11] This finding prompts additional questions. First, does bipyridyl-treated Dps-HE emulate Dps-1 in terms of metal-dependent DNA binding? Second, can any metal restore DNA binding to bipyridyl-treated Dps-1? Can the metals restore DNA binding in any condition, such as during oxidative stress? Finally, is there a preference for a particular metal at the metal binding sites? To address the first question, an EMSA was conducted with bipyridyl-treated Dps-HE to which divalent metal was subsequently added. Results show that bipyridyl-treated Dps-HE lost its ability to bind DNA (Figure 6, lane 2) and that the addition of Mn(II) restored DNA binding (Figure 6, lane 3). This is similar to the previous finding with Dps-1, except that bipyridyl-mediated removal of metal from wild-type Dps-1 does not alter oligomeric state, whereas hexameric Dps-HE disassembles following incubation with bipyridyl (Figure 3d).[11]

To address the subsequent questions, EMSAs were conducted using different metals. Co(II) was used because it was seen to bind at all metal-binding sites in the crystal structure of Dps-1,[20] Fe(II) was chosen because Dps is an iron storage protein,[25] and Mn(II) was selected due to the high Mn:Fe ratio in *D. radiodurans*.[16] Results confirm that removal of metals from Dps-1 by treatment with bipyridyl abolishes DNA binding (Figure 7a, lanes 2−4), suggesting that metal binding is needed to orient the N-terminus in a way that allows it to bind DNA (an inference based on retention of the dodecameric superstructure and the absolute requirement for the N-terminal extensions for DNA binding).[11] Conversely, addition of either Co(II), Fe(II), or Mn(II) to bipyridyl-treated Dps-1 restores DNA binding (Figure 7a, lanes 5−13). Notably, Fe(II) fails to restore DNA binding to Dps-1 in the presence of hydrogen peroxide, conditions under which Dps-1 would also

dx.doi.org/10.1021/bi300703x | *Biochemistry* 2012, 51, 6679−6689

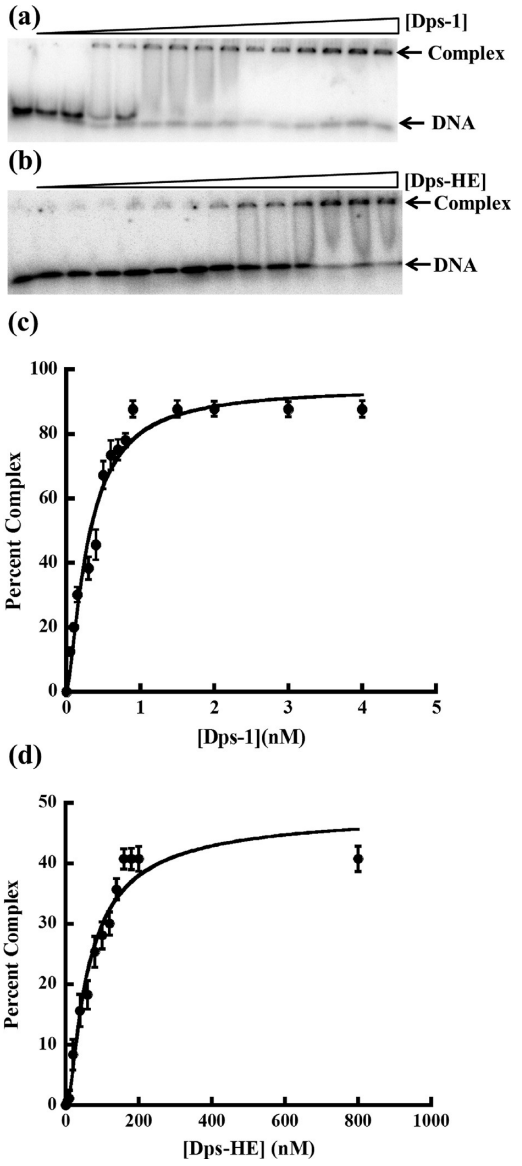

Figure 5. DNA binding by wild-type Dps-1 and Dps-HE. Electrophoretic analysis of 26 bp duplex DNA with Dps-1 (a) and Dps-HE (b) under equilibrium conditions ([DNA] < K_d). For Dps-1, concentrations range from 0 to 4 nM dodecamer. For the mutant Dps-HE, concentrations range from 0 to 800 nM hexamer. (c) Binding isotherm for Dps-1 binding to 26 bp DNA. (d) Binding isotherm for Dps-HE binding to 26 bp DNA. The Hill equation was used to obtain the best fit data (R^2 = 0.9677, n = 1.4 ± 0.1 for Dps-1 and R^2 = 0.9726, n = 0.7 ± 0.1 for Dps-HE).

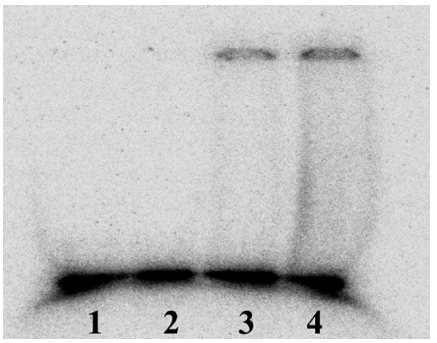

Figure 6. Effect of metal on DNA binding by bipyridyl-treated Dps-HE. DNA is incubated without Dps-HE (lane 1), 60 nM bipyridyl-treated Dps-HE (lane 2), 60 nM bipyridyl-treated Dps-HE followed by the addition of 1 μM $MnCl_2$ (lane 3) and 60 nM of untreated Dps-HE (lane 4). Equivalent results obtained with 400 nM Dps-HE (data not shown).

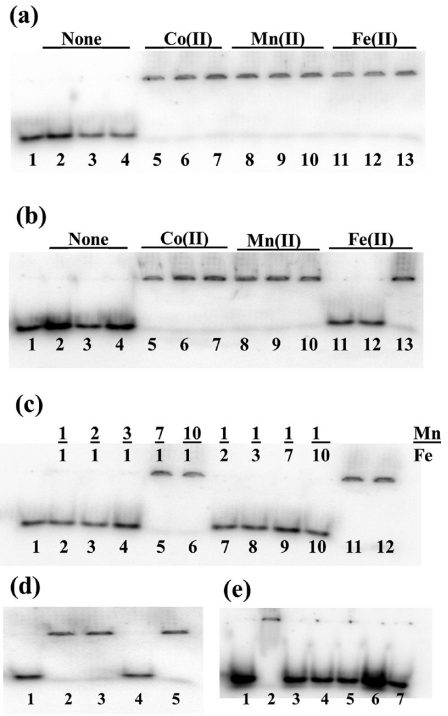

Figure 7. Effect of different metals on DNA binding by bipyridyl-treated Dps-1. (a) DNA incubated with increasing concentration of bipyridyl-treated Dps-1 (1−10 nM); lanes 2−4, in the absence of metal; lanes 5−7, with 80 nM $CoCl_2$; lanes 8−10, with 80 nM $MnCl_2$; lanes 11−13, with 80 nM $Fe(NH_4)_2(SO_4)_2$. (b) Same reactions as (a) with the addition of 1 mM H_2O_2 (lanes 2−13). (c) Competition assay between Mn and Fe in the presence of H_2O_2. Lane 2 has equal ratio of Mn:Fe, lanes 3−10 have varying ratio of Mn:Fe (2:1, 3:1, 7:1; 10:1, 1:2, 1:3, 1:7, and 1:10), lane 11 contains Mn only, and lane 12 contains Fe only. Reactions in lanes 2−10 contain 1 mM of H_2O_2, and reactions in lanes 2−12 contain 1 nM Dps-1. (d) Recovery assay using Mn(II). DNA binding of 1 nM bipyridyl-treated Dps-1 with Fe(II) (lane 2), Mn(II) (lane 3), Fe(II) with H_2O_2 (lane 4) and Fe(II) with H_2O_2 followed by addition of Mn(II) (lane 5). (e) Metal effect on DNA migration. Lane 2, Dps-1 with Fe(II); lane 3, Dps-1 with Fe(III); lane 4, Fe(II) only; lane 5, Fe(III) only; lane 6, Mn(II) only; lane 7, Co(II) only. In all five panels, the first lane corresponds to free DNA.

exhibit ferroxidase activity (Figure 7b, lanes 11 and 12). It is only at a high concentration of Dps-1 that DNA binding is restored in the presence of peroxide (Figure 7b, lane 13; this reaction corresponds to a condition where the concentration of N-terminal binding sites (120 nM) exceeds that of Fe^{2+} (80 nM)). In contrast, H_2O_2 has no effect on DNA binding in the presence of Co(II) and Mn(II) (Figure 7b, lanes 5−10). Since different metals can bind at the metal sites, and given the high Mn:Fe ratio characteristic of *D. radiodurans*, we investigated if there is a preference for a particular metal using a competition assay. At equal ratio of Mn:Fe, DNA binding is not restored to bipyridyl-treated Dps-1 in the presence of peroxide (Figure 7c, lane 2). When the [Mn] is much higher (Mn:Fe is 7:1), DNA binding is restored (Figure 7c, lane 5). This suggests the occurrence of redox reactions that reduce the concentration of Mn(II) available to bind the site when Fe(II) is being oxidized

dx.doi.org/10.1021/bi300703x | *Biochemistry* 2012, 51, 6679−6689

by H_2O_2 (and expected due to the higher reduction potential of Mn).

Since Fe(II) cannot restore DNA binding to bipyridyl-treated Dps-1 in the presence of peroxide, this suggests two possibilities. First, when Fe(II) binds to the N-terminal metal sites with peroxide present, the histidine residues that coordinate that site might get oxidized. A study by Lee and Helmann shows that the transcriptional regulator PerR fails to bind DNA when Fe(II) is bound at the metal site in the presence of peroxide. They also show that the loss of DNA binding is due to the histidine residues that coordinate the metal getting oxidized. The oxidation of those histidines prevents any metal from binding.[26] Second, peroxide might oxidize Fe(II) to Fe(III), which can no longer bind at the site. To address which scenario is correct, a recovery assay was conducted in which Mn(II) was added to Fe(II)-treated Dps-1 in the presence of peroxide. As shown in Figure 7d, when Mn(II) is added to Dps-1 after Fe(II), DNA binding is restored (lane 5) compared to the lack of DNA binding when Dps-1 is incubated with Fe(II) and H_2O_2 (lane 4) or with Fe(III) (Figure 7e, lane 3). This suggests that it is most likely the Fe(II) that is being oxidized as His-oxidation would have resulted in reduced metal binding and hence significantly attenuated DNA binding (Figure 5b). Finally, to rule out that the metals affect the migration of the DNA, an EMSA was carried in which the metals (Fe(II), Fe(III), Mn(II), and Co(II)) were incubated with free DNA. Results show that the metals have no effect on DNA migration (Figure 7e).

Mn(II) Inhibits Ferroxidase Activity. For some Dps homologues, certain metals can inhibit ferroxidase activity. For example, Zn(II) has been shown to block ferroxidase activity by competing with Fe(II) for binding at the ferroxidase site.[27] *D. radiodurans* accumulates a high level of Mn(II); therefore, we determined the effect of this metal on ferroxidase activity. Using equivalent concentrations of monomer, each protein sample contains the same concentration of ferroxidase centers (but not the same molar concentration of dodecamer or hexamer, respectively). Both Dps-1 and Dps-HE exhibit ferroxidase activity, consistent with a hexameric assembly of Dps-HE containing three ferroxidase centers. Interestingly, there appears to be a delay at the start of the ferroxidation reaction for Dps-HE before a gradual increase in absorbance is visible, perhaps reflecting assembly issues that are delaying the ferroxidase activity of this mutant. However, the ferroxidase activity of both Dps-1 and Dps-HE is completely abolished in the presence of Mn(II), suggesting that Mn(II) competes for binding to the ferroxidase center (Figure 8).

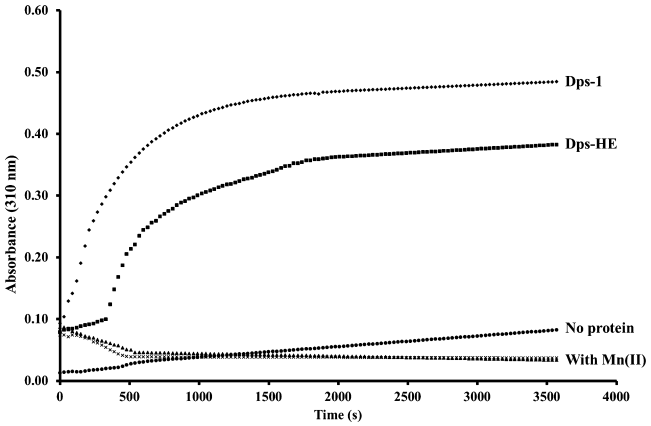

Figure 8. Effect of Mn(II) on ferroxidase activity of Dps-1 and Dps-HE. Iron oxidation by Dps-1 and Dps-HE in 20 mM MOPS buffer. The concentration of both protein were 0.2 mg/mL. The kinetics of iron oxidation by Dps-1 and air were measured at 310 nm. Ferroxidase activity of Dps-1 with Fe(II) (diamond), Dps-HE with Fe(II) (square), Fe(II) only (circle), Dps-1 with Fe(II) and Mn(II) (triangle), and Dps-HE with Fe(II) and Mn(II) (×).

DISCUSSION

Ferroxidase Activity of Dps-1 May Be Prevented *in Vivo*. Mn(II) inhibits ferroxidase activity of both Dps-1 and Dps-HE at a Mn:Fe ratio of 0.2, comparable to the ratio reported in *D. radiodurans*.[16] This inhibition is likely due to Mn(II) binding at the ferroxidase site. Although we cannot rule out the possibility that Mn(II) binds other sites, resulting in an altered conformation of the ferroxidase center, this is unlikely for a couple of reasons. First, altering the metal site at the N-terminus has little impact on the ferroxidase activity (Figure 8). This is also evidenced by a previous report that Dps-dn, the mutant that lacks the entire N-terminus, exhibits ferroxidase activity.[11] Second, mutations in the metal site at the iron exit channel did not affect the ferroxidase activity or the core formation of Dps-1.[20] Therefore, even if Mn(II) binds at those sites, it would not be expected to affect the ferroxidase activity. *D. radiodurans* accumulates manganese, which is globally distributed, and it sequesters iron in a region overlapping the septum between dividing cells.[17] Dps-1 is associated with the nucleoid.[28] The physiological implication, therefore, is that ferroxidase activity of Dps-1 may be prevented in a cellular environment where [Mn] > [Fe] (Figure 9).

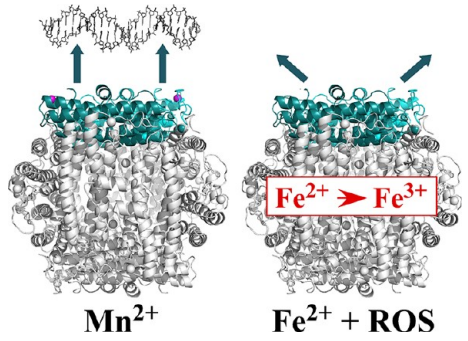

Figure 9. Model of Dps-1 function. Left panel indicates Dps-1 binding to DNA under normal physiological conditions where [Mn^{2+}] > [Fe^{2+}]. One Dps-1 dimer is shown in cyan with metal bound at the N-terminal metal site in magenta. Arrows represent N-terminal extensions interacting with DNA major grooves. When Fe^{2+} and ROS are present, Dps-1 catalyzes the oxidation of Fe^{2+} to Fe^{3+} to prevent hydroxyl radical formation by Fenton chemistry, but with the potential for iron subsequently leaving the mineral core. Without metal bound at the N-terminal metal site, the N-terminal extensions are not structured properly for DNA interaction.

The N-Terminal Metal Site Affects DNA Binding. Dodecameric Dps-1 may be thought of as composed of six dimers, each composed of two subunits oriented in an antiparallel fashion.[20,21] DNA binding has been proposed to involve contact with the N-terminal extensions protruding from either end of a dimer and with Arg132 in the short helix between the second and third helix of the four-helix bundle subunit (Figure 9, left panel).[11,29] Positive cooperativity of DNA binding by Dps-1 is seen only with dodecameric protein, which features six DNA sites,[29] and not with dimeric Dps-1 or

dx.doi.org/10.1021/bi300703x | *Biochemistry* 2012, 51, 6679−6689

hexameric Dps-HE, pointing to conformational changes on DNA binding to dodecameric protein that propagate to other DNA sites. Dimeric Dps-1 features only one DNA site, while the lack of cooperativity of DNA binding by Dps-HE, which would be expected to have three DNA sites, suggests that the connectivity between DNA sites that is evidenced by the positive cooperativity of DNA binding by dodecameric Dps-1 is lost in Dps-HE, perhaps related to its suboptimal assembly.

DNA binding by Dps-HE is significantly reduced (Figure 5). Dodecameric Dps-1 has been shown to feature six DNA sites, with N-terminal extensions preceding the metal site required for DNA binding, along with Arg132 in the middle of the four-helix bundle subunit.[29] This suggests that DNA binds with its axis parallel to the dimer interface. If hexameric assembly of Dps-HE were the only difference compared to dodecameric Dps-1, with individual DNA sites otherwise remaining unaltered, a change in DNA-binding affinity reflecting half the number of DNA sites would be expected for Dps-HE. Instead, we observe a >100-fold decrease in affinity. An interpretation more consistent with the observed change in DNA binding is therefore that metal-coordination aids in structuring the N-termini, thereby mediating optimal DNA contacts. Since a Dps-1 mutant containing the N-terminal metal site but lacking the flexible N-terminal extension fails to bind DNA, the metal site is likely required only for structuring the N-terminus and not for direct DNA contacts. However, as for Dps-1, DNA binding by Dps-HE is metal-dependent. Inspection of the Dps-1 sequence suggests the presence of several alternate metal-coordinating residues in the N-terminus. For example, Glu21, Asp33, His34, His51, Glu54, and Glu57 might be able to participate in this coordination; as there are several His and Glu residues in the N-terminus that could substitute for the His and Glu that were mutated in Dps-HE, the chemistry of coordination is likely unaltered. If the original metal site is disrupted and a metal is coordinated by other residues, then that would change the conformation of the loop as well as the disposition of the N-terminus. As a result, the N-terminal extension may not be oriented such that optimal DNA binding can occur. That removal of metals by bipyridyl treatment led to a complete loss of DNA binding for both Dps-1 and Dps-HE is likely due to excessive flexure of the N-terminal extension.

Differential Metal Effects on DNA Binding. Experiments with bipyridyl-treated Dps-1 show that different metals ((Co(II), Mn(II), and Fe(II)) can restore DNA binding to metal-free Dps-1. Notably, Fe(II) is unable to restore DNA binding in the presence of hydrogen peroxide. Since addition of Mn(II) to the peroxide-treated, Fe(II)-bound Dps-1 restores DNA binding, Fe(II) is likely oxidized to Fe(III), which cannot bind the metal site (Figure 7). We also note that since Dps-1 binds DNA in the presence of Fe^{2+} (Figure 7a), the interpretation is that Fe^{2+} already bound is protected from oxidation by molecular oxygen on the time scale of the DNA-binding assay, but not from oxidation by H_2O_2. The physiological relevance of this observation is that Dps-1 may be prevented from binding DNA under conditions of ongoing ferroxidation, conditions that might also lead to subsequent release of iron from the core and the consequent production of $^{\bullet}OH$ through Fenton chemistry (Figure 8). Thus, differential metal binding at the N-terminal metal site provides a possible mechanism by which the two functions of Dps-1 may be separated to prevent $^{\bullet}OH$-mediated damage to Dps-1-bound DNA.

Proposed Assembly of Hexameric Dps-HE. Dps-1 exists almost exclusively as a dodecamer. Only at low salt concentrations can dimeric Dps-1 be detected following expression in *E. coli*.[19] No monomer may be detected, even for Dps-dn that lacks the entire N-terminal extension.[11] This is consistent with the PISA algorithm, which uses thermodynamics calculations to predict which assemblies are likely to be most stable in solution; PISA predicts that both protein−protein contacts at the dimer interface as well as metal coordination at the ferroxidase center contribute significantly to thermodynamic stability of the dodecameric superstructure (Table 2). As these contacts would also be present in dimeric Dps-1, it is reasonable to infer that this interface is responsible for stability of the Dps-1 dimer. Assembly of dodecameric Dps-1 is therefore likely to occur by association of six dimers. This is different from the reported assembly of *M. smegmatis* Dps1, for which trimers were suggested to be assembly intermediates.[12,30] That disruption of the N-terminal metal site to generate Dps-HE compromises assembly clearly shows that proper conformation of the metal-bound loop is a prerequisite for dodecamer formation (Figure 3). The structure of Dps-1 shows that the metal-bound loop contacts a neighboring dimer, and evaluation of Dps-1 using PISA also points to this interface participating significantly in assembly; for instance, His51 within the loop forms a salt bridge with Asp191 of the adjacent subunit and Tyr52 forms a hydrogen bond to Arg165.[20] Consistent with the important contribution of such interactions, we also note that Arg165 corresponds to one of two residues that when substituted together in *E. coli* Dps prevent dodecamer formation.[31] That metals may be removed from dodecameric Dps-1 without effect on oligomeric state, but with severe consequences to DNA-binding, also suggests that contacts between the metal-bound loop and the adjacent dimer are destabilized on removal of metal, but no longer needed to maintain the oligomeric state. The destabilization predicted by PISA analyses to result from removal of metals is evident in the significantly reduced thermal stability of bipyridyl-treated Dps-1 (Figure 2). Taken together, our data suggest that occupancy of the N-terminal metal site is required for initial contacts between associating dimers, but not to maintain the dodecameric assembly once attained.

For Dps-HE, the N-terminal loops are not properly folded, which means that optimal interactions between adjacent dimers cannot occur. The outcome is a hexameric assembly that is incompatible with further assembly into a dodecamer. The delay at the start of the ferroxidation reaction with Dps-HE likely also reflects its suboptimal assembly, since the ferroxidase center resides between two subunits. That Dps-HE does not exist as a dimer in the presence of divalent metal suggests that alternate residues coordinate the metal, as discussed above. This is also supported by the previous observation that a mutant Dps-1 in which the first 33 amino acids are removed could not form a dodecamer unless the N-terminal His-tag was cleaved. This finding suggests that the extra histidine residues interfered with proper metal coordination to prevent oligomerization.[11] Evidently, coordination of metal by alternate residues promotes some interaction between dimers to yield the observed hexamer.

Dps-1 contains two types of 3-fold axes that pass through either the iron entry or exit channels: the ferritin-like and Dps-like axes, respectively (Table 1). There is a metal site at the iron entry channel, and this metal is coordinated by Asp181 from three subunits. In one of the two published Dps-1 structures, this site is not filled unless the crystals are soaked in a solution containing Fe^{2+}.[21] This suggests that occupancy of this site is

dx.doi.org/10.1021/bi300703x | *Biochemistry* 2012, 51, 6679−6689

unnecessary for dodecameric assembly. Likewise, a metal near the iron exit channel is also coordinated by residues from three subunits. However, for the metal site at the iron exit channel to have a structural role is also unlikely since mutations in this site did not affect dodecameric assembly.[20] Considering the building blocks of dodecameric Dps-1 to be a dimer, a hexamer centered around the iron entry site would be primarily stabilized by the N-terminal loops interacting with the neighboring dimer, while a hexamer assembled around the 3-fold axis that passes through the iron exit site would in addition be stabilized by protein−protein contacts between adjoining subunits and the embedded sulfate ion. Consistent with the contribution of these interfaces, PISA analysis predicts that a trimer assembled around the exit pore would be more stable than one assembled around the entry site. We therefore propose that the Dps-HE hexamer may correspond to three dimers assembled about the iron exit (Dps-like) channel.

In conclusion, our data show that metal binding at the N-terminus is required to initiate dodecameric assembly and that incomplete structuring of the N-terminal loop leads to a hexameric assembly intermediate. After assembly, metal binding is no longer required to maintain the oligomeric state; instead, it impacts DNA interactions, particularly under conditions of oxidative stress. This affords a mechanism by which DNA-binding is avoided under conditions where Dps-1 would engage in ferroxidation. Combined with the efficient inhibition of ferroxidation by Mn(II) at the Mn:Fe ratio observed in *D. radiodurans*, this regulation may serve to separate the two functions of Dps-1 to prevent damage to Dps-1-bound DNA deriving from iron leaking from the core followed by generation of $^{\bullet}$OH through Fenton chemistry.

AUTHOR INFORMATION

Corresponding Author

*Tel 225-578-5148; Fax 225-578-8790; e-mail agrove@lsu.edu.

Funding

Research was supported by the National Science Foundation (MCB-0744240 and 1051610 to A.G.)

Notes

The authors declare no competing financial interest.

ABBREVIATIONS

Dps, DNA protection during starvation; EMSA, electrophoretic mobility shift assay; IPTG, isopropyl-β-D-thiogalactopyranoside; PAR, 4-(2-pyridylazo)resorcinol; PISA, protein interfaces, surfaces, and assemblies; PMSF, phenyl methyl sulfonyl fluoride; ROS, reactive oxygen species.

REFERENCES

(1) Imlay, J., and Linn, S. (1988) DNA damage and oxygen radical toxicity. *Science 240*, 1302−1309.

(2) Crichton, R., Wilmet, S., Legssyer, R., and Ward, R. (2002) Molecular and cellular mechanisms of iron homeostasis and toxicity in mammalian cells. *J. Inorg. Biochem. 91*, 9−18.

(3) Imlay, J. (2008) Cellular defense against superoxide and hydrogen peroxide. *Annu. Rev. Biochem. 77*, 755−776.

(4) Almirón, M., Link, A. J., Furlong, D., and Kolter, R. (1992) A Novel DNA-binding protein with regulatory and protective roles in starved *Escherchia coli*. *Genes Dev. 6*, 2646−2654.

(5) Martinez, A., and Kolter, R. (1997) Protection of DNA during oxidative stress by the nonspecific DNA-binding protein Dps. *J. Bacteriol. 179*, 5188−5194.

(6) Zhao, G., Ceci, P., Ilari, A., Giangiacomo, L., Laue, T. M., Chiancone, E., and Chasteen, N. D. (2002) Iron and hydrogen peroxide detoxification properties of DNA-binding protein from starved cells. *J. Biol. Chem. 277*, 27689−27696.

(7) Su, M., Cavallo, S., Stefanini, S., Chiancone, E., and Chasteen, N. D. (2005) The so-called *Listeria innocua* ferritin is a Dps protein. Iron incorporation, detoxification, and DNA protection properties. *Biochemistry 44*, 5572−5578.

(8) Harrison, P. M., and Arosio, P. (1996) The ferritins: molecular properties, iron storage function and cellular regulation. *Biochim. Biophys. Acta 1275*, 161−203.

(9) Grant, R., Filman, D., Finkel, S., Kolter, R., and Hogle, J. (1998) The crystal structure of Dps, a ferritin homolog that binds and protects DNA. *Nat. Struct. Biol. 5*, 294−303.

(10) Stillman, T. J., Upadhyay, M., Norte, V. A., Sedelnikova, S. E., Carradus, M., Tzokov, S., Bullough, P. A., Shearman, C. A., Gasson, M. J., Williams, C. H., Artymiuk, P. J., and Green, J. (2005) The crystal structures of *Lactococcus lactis* MG1363 Dps proteins reveal the presence of an N-terminal helix that is required for DNA binding. *Mol. Microbiol. 57*, 1101−1112.

(11) Bhattacharyya, G., and Grove, A. (2007) The N-terminal extensions of *Deinococcus radiodurans* Dps-1 mediated DNA major groove interactions as well as assembly of the dodecamer. *J. Biol. Chem. 282*, 11921−11930.

(12) Roy, S., Saraswathi, R., Gupta, S., Sekar, K., Chatterji, D., and Vijayan, M. (2007) Role of N and C-terminal tails in DNA binding and assembly in Dps: structural studies of *Mycobacterium smegmatis* Dps deletion mutants. *J. Mol. Biol. 370*, 752−767.

(13) Mattimore, V., and Battista, J. R. (1996) Radioresistance of *Deinococcus radiodurans*: functions necessary to survive ionizing radiation are also necessary to survive prolonged desiccation. *J. Bacteriol. 178*, 633−637.

(14) Battista, J. R. (1997) Against all odds: the survival strategies of *Deinococcus radiodurans*. *Annu. Rev. Microbiol. 51*, 203−224.

(15) Cox, M. M., and Battista, J. R. (2005) *Deinococcus radiodurans* - the consummate survivor. *Nat. Rev. Microbiol. 3*, 882−892.

(16) Daly, M. J., Gaidamakova, E. K., Matrosova, V. Y., Vasilenko, A., Zhai, M., Venkateswaran, A., Hess, M., Omelchenko, M. V., Kostandarithes, H. M., Makarova, K. S., Wackett, L. P., Fredrickson, J. K., and Ghosal, D. (2004) Accumulation of Mn(II) in *Deinococcus radiodurans* facilitates gamma-radiation resistance. *Science 306*, 1025−1028.

(17) Daly, M. J., Gaidamakova, E., Matrosova, V., Vasilenko, A., Zhai, M., Leapman, R., Lai, B., Ravel, B., Li, S., Kemner, K., and Fredrickson, J. (2007) Protein oxidation implicated as the primary determinant of bacterial radioresistance. *PLoS Biol. 4*, e92.

(18) Makarova, K. S., Aravind, L., Wolf, Y. I., Tatusov, R. L., Minton, K. W., Koonin, E. V., and Daly, M. J. (2001) Genome of the extremely radiation-resistant bacterium *Deinococcus radiodurans* viewed from the perspective of comparative genomics. *Microbiol. Mol. Biol. Rev. 65*, 44−79.

(19) Grove, A., and Wilkinson, S. P. (2005) Differential DNA binding and protection by dimeric and dodecameric forms of the ferritin homolog Dps from *Deinococcus radiodurans*. *J. Mol. Biol. 347*, 495−508.

(20) Kim, S. G., Bhattacharyya, G., Grove, A., and Lee, Y. H. (2006) Crystal structure of Dps-1, a functionally distinct Dps protein from *Deinococcus radiodurans*. *J. Mol. Biol. 361*, 105−114.

(21) Romão, C. V., Mitchell, E. P., and McSweeney, S. M. (2007) The crystal structure of *Deinococcus radiodurans* Dps protein (DR2263) reveals the presence of a novel metal centre in the N terminus. *J. Biol. Inorg. Chem. 11*, 891−902.

(22) Krissinel, E., and Henrick, K. (2007) Inference of macromolecular assemblies from crystalline state. *J. Mol. Biol. 372*, 774−797.

(23) Gupta, S., and Chatterji, D. (2003) Bimodal protection of DNA by *Mycobacterium smegmatis* DNA-binding protein from stationary phase cells. *J. Biol. Chem. 278*, 5235−5241.

(24) McCall, K., and Fierke, C. (2000) Colorimetric and fluorimetric assays to quantitate micromolar concentrations of transition metals. *Anal. Biochem. 284*, 307−315.
(25) Ilari, A., Ceci, P., Ferrari, D., Rossi, G. L., and Chiancone, E. (2002) Iron incorporation into *Escherichia coli* Dps gives rise to a ferritin-like microcrystalline core. *J. Biol. Chem. 277*, 37619−37623.
(26) Lee, J. W., and Helmann, J. D. (2006) The PerR transcription factor senses H_2O_2 by metal catalyzed histidine oxidation. *Nature 440*, 363−367.
(27) Stefanini, S., Cavallo, S., Montagnini, B., and Chiancone, E. (1999) Incorporation of iron by the unusual dodecameric ferritin from *Listeria innocua*. *Biochem. J. 338*, 71−75.
(28) Nguyen, H. H., de la Tour, C. B., Toueille, M., Vannier, F., Sommer, S., and Servant, P. (2009) The essential histone-like protein HU plays a major role in *Deinococcus radiodurans* nucleoid compaction. *Mol. Microbiol. 73*, 240−252.
(29) Nguyen, K. H., Smith, L. T., Xiao, L., Bhattacharyya, G., and Grove, A. (2012) On the stoichiometry of *Deinococcus radiodurans* Dps-1 binding to duplex DNA. *Proteins 80*, 713−721.
(30) Chowdhury, R. P., Vijayabaskar, M. S., Vishveshwara, S., and Chatterji, D. (2008) Molecular mechanism of in vitro oligomerization of Dps from *Mycobacterium smegmatis*: mutations of the residues identified by "interface cluster" analysis. *Biochemistry 47*, 11110−11117.
(31) Zhang, Y., Fu, J., Chee, S. Y., Ang, E. X., and Orner, B. P. (2011) Rational disruption of the oligomerization of the mini-ferritin *E. coli* DPS through protein-protein interface mutation. *Protein Sci. 20*, 1907−1917.